УДК 629.05

DOI: https://doi.org/10.20535/0203-3771422021268467

O. Petrenko[1], **V. Chikovani**[2], *д.т.н., професор*,
S. Golovach[3], *к.т.н., головний конструктор*, **G. Strokatch**[4]

EXPERIMENTAL INVESTIGATION OF THE MAXIMUM QUALITY FACTOR AXES TEMPERATURE DEVIATION IN METALLIC CORIOLIS VIBRATORY GYROSCOPES RESONATOR

Ua Металевий циліндричний резонатор є загальновідомою базовою деталлю значної частини вібраційних гіроскопів Коріоліса (*CVG*) [1], у тому числі гіроскопа *MEMS*. Його власні параметри відразу після механічного виготовлення в основному визначають доцільність подальшого використання та майбутній потенціал точності гіроскопа. Початкові випробування *CVG* резонаторів безпосередньо після їх виготовлення часто проводять оптичним методом [2, 3] або акустичним методом [4, 5]. На жаль, досліджена якість виготовлення резонаторів за допомогою акустичного методу не дуже добре описана в науковій літературі. У статті представлено результати деяких розширених акустичних досліджень металевих *CVG* резонаторів. Цей результат описує поведінку осей максимального коефіцієнта якості (*Q*-фактор) і осей власних резонансних частот під впливом стабілізованих температурних кроків і може бути використаний для прогнозування для мінімізації зміщення *CVG* під час його роботи в діапазоні температур.

En A metallic cylindrical resonator is a well-known base detail of the significant part of Coriolis vibratory gyroscopes (CVG) [1] including a MEMS gyro. It own parameters just after mechanical manufacture in main are determine an advisability of further utilize and the future gyroscope accuracy potential. Initial testing CVG resonators directly after their manufacture often done using the optical method [2, 3] or acoustic method [4, 5]. Unfortunately investigated manufacture quality of the resonators by using acoustic method not very well describe in scientific literature. A paper presents the results of some extension acoustic investigations of the metallic CVG resonators. This result describes the behavior of maximum quality factor (*Q*-factor) axes and own resonant frequencies axes under stabilized temperature step influences and can be used in prediction for CVG bias minimization during it works in temperature range.

Metallic resonator parameters observed

The metallic cylindrical resonators that observed in this paper related to CVG with high accuracy performances [6]. Such resonator making from elinvar steel alloys and have a diameter about 43 mm and it model demonstrated

[1] *Igor Sikorsky Kyiv Polytechnic Institute*
[2] *National Aviation University*
[3] *Public joint stock company Elmiz*
[4] *Igor Sikorsky Kyiv Polytechnic Institute*

on Fig. 1. Initial testing CVG resonators by using acoustic method immediately after it manufacturing provide determination mainly such parameters as resonance frequency mismatch, *Q*-factor and coefficient of resonance frequency thermal dependency. These parameters are important for understanding the possible time cost for future balancing operations and potential CVG accuracy characteristics in temperature range. According to the latest investigations of controlling standing wave angular position in CVG exist an optimal excitation angle where the bias error can significantly reduce [7]. In turn the optimal excitation angle is very closely related with axis of minimal damping or maximum *Q*-factor that finally determined during balancing operations. But considering that the process of the maximum *Q*-factor axis temperature deviation still remains poorly studied this paper focus on these investigations.

Fig. 1. Metallic CVG resonator which was investigated

As well-known main part of CVG errors on base of metallic cylindrical resonator is caused by material heterogeneous disposal and technological errors during manufacture. Maximal influence for second (operational) resonator oscillation mode has fourth harmonic of Fourier transform of mass imbalance [8]. As a result of such harmonic existence, the natural frequency of the resonator oscillates is split into two frequencies. The fourth harmonic of the mass distribution along the rim of the resonator gives the following values of frequency splitting:

$$\Delta\omega = \varepsilon \cdot \frac{\omega 2}{2}, \qquad (1)$$

where ε is a relative defect value (Δm/m) on fourth harmonic.

On Fig. 2 shown a simple model of cylinder resonator vibrational mass distribution with dominant imbalance mass component on fourth harmonic. Fourth harmonic of mass imbalance cause to existence in resonator two axis that biased with respect to each other on 45° and the own frequencies along this axis has maximum and minimum respectively. Two different frequencies existence cause to displace a standing wave by his nodes between axes for second mode that shown on Fig. 2.

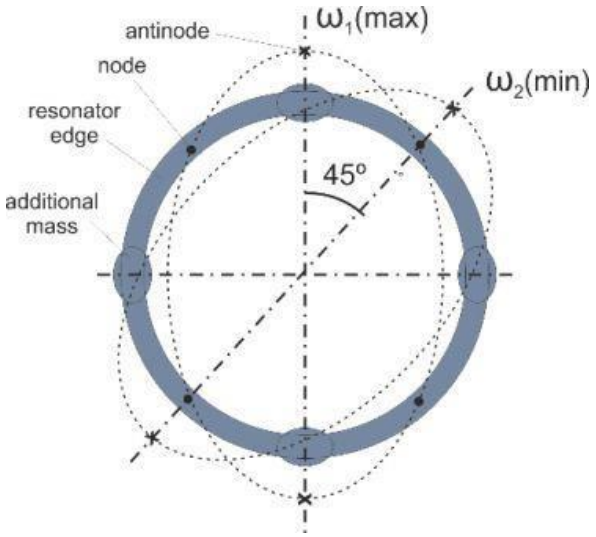

Fig. 2. Frequency split under fourth harmonic of mass distribution

To determine on this mode the resulting standing wave motion random location it is necessary to decompose the oscillations of the wave into components along the normal (own) axes ω_1 and ω_2. Since these components are oscillate with different frequencies, it should first be noted that the composite standing wave ceases to be a standing wave because appear component of the traveling wave. This can also be explained by the fact that a quadrature component of the secondary wave is created, the antinodes of which coincide with the nodes of the primary wave, oscillating with the quadrature phase with respect to the primary wave with a phase angle of 90°. In this case there is a so-called standing wave the speed of which is determined by the following expression

$$\dot{\theta} = \frac{1}{8}(\Delta\omega)^2 t \cdot \sin 4\varphi_o \,, \tag{2}$$

where φ_o is an angle between of oscillation direction and one of the own axes, $\Delta\omega = \omega_1 - \omega_2$ – is a frequency split own resonant frequency of a resonator. From (2) we can see that under $\varphi_0 = 0, \pi/4$, when direction of oscillations is coincide with one of the own axes of resonator oscillations will be represent by clean standing wave. For second harmonic of a resonator the density defect of material is determined by next expression:

$$\rho = \rho_0(1 + \varepsilon_2 \cos 2\varphi) \,. \tag{3}$$

And the value estimation of a frequency split is determined by expression [9, 10]:

$$\Delta\omega = \frac{8}{5}\varepsilon_2^2\omega_2. \tag{4}$$

As we can see from (3) and (4) values of frequency split is a second order of smallness relate to second harmonic of a resonator the density defect. It

necessary to note that frequency split for first and third harmonic of the defect also give a second order of smallness value. Hence it necessary to paid main attention on fourth harmonic of a resonator defect during it manufacture, because this harmonic have much more influence to CVG errors that another.

Another significant reason of the error in output CVG signal is inhomogeneous sources of damping oscillations distribution in resonator (due to inhomogeneous it material). Like in case of thickness of resonator edge variation, as was described above, the fourth harmonic of damping distribution also cause to frequency split.

Damping material have property of a resonator oscillation braking proportional to it radial shape velocity in direction of damping source. Such a standing wave with its antinodes that placed in damping sources will be have a lower Q-factor (i. e. lower time τ of amplitude attenuation in e times, because) $Q = \omega\tau/2)$ than standing wave with its nodes that placed in damping sources. For standing wave drift understanding it need to decomposition it to components along two main damping axes (solid and dash-dot lines on Fig. 3). Amplitudes of this two components are decreased with $1/\tau_1$ and $1/\tau_2$ relatively. While resonator mounting in CVG construction a ring electrode reinforce this components with same speed that it decrease. In the same time an amplitude in operating loop support a square root from sum of the amplitudes square on a set value (i.e. $= \sqrt{(A_1)^2 + (A_2)^2}$). In this conditions components with lower damping time are completely decrease and a standing wave is eventually set on axis with lower damping time τ_1.

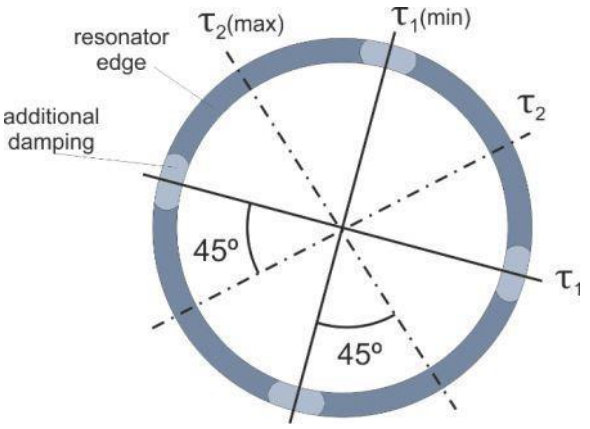

Fig. 3. Fourth harmonic of damping distribution

In CVG construction under X drive electrode excitation (Fig. 4) standing wave angular position θ with respect to the drive electrode is calculated by the well-known expression [8]:

$$\theta = \frac{1}{2} a \cdot \mathrm{tg} \frac{A_n}{A_{an}} , \qquad (5)$$

where A_n is node signal amplitude; A_{an} is antinode signal amplitude. As was described above antinode signal amplitude is stabilized at predetermined value, and node signal amplitude under absent of angle rate and compensating feedback control signal is determined by resonator's imperfections. The node signal amplitude An can be determined by solution of the following differential equation [11]:

$$\ddot{y} + \frac{2}{\tau}\dot{y} + \omega_2^2 y = \left[A_{an}\omega_1 \Delta\left(\frac{1}{\tau}\right)\sin 2\theta_\tau \right]\sin\omega_1 t + \\ + (A_{an}\omega\Delta\omega\sin 2\theta_\omega)\cos\omega_1 t \quad , \qquad (6)$$

where $\Delta\left(\frac{1}{\tau}\right) = \frac{1}{\tau_1} - \frac{1}{\tau_2}$; $\omega\Delta\omega = \frac{\omega_1^2 - \omega_2^2}{2}$; is a resonator displacement from initial position along y direction (Fig. 4) during vibration; τ_1, τ_2 are minimum and maximum damping constants, respectively; ω_2 is a resonant frequency along *Y* direction; ω_1 is a resonant frequency along *X* direction; θ_τ is an angle between standing wave antinode and minimum damping axis; θ_ω is an angle between standing wave antinode and minimum frequency axis; ω_1, ω_2 are maximum and minimum resonant frequencies, respectively. Expression 11 perfectly demonstrates how the mass rebalance (second part of the right side expression) and the heterogeneity (first part of the right side expression) in total affect on bias error in CVG.

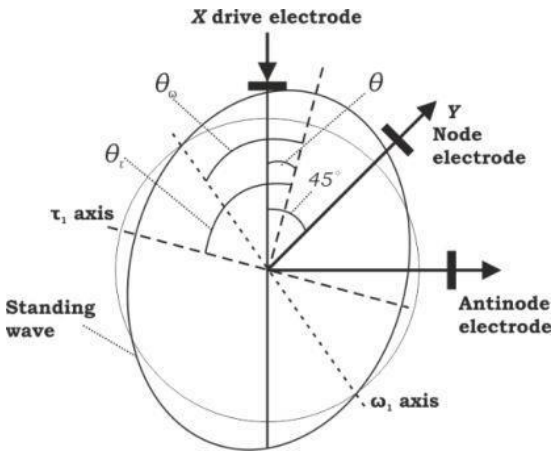

Fig. 4. Standing wave excited by *X* drive electrode in non-ideal resonator

There were consider some main relations between the standing wave angular position and the values of *Q*-factor and frequency mismatches. Next part of this work aim to obtain an experimental observations of this relationships with help of acoustic testing method.

Methodology for maximum and minimum *Q*-factor and resonant frequency axes determination

As has been mentioned above, for investigation of a metallic CVG resonator used acoustic methodology. This methodology is used in CVG early-stage production and it base principals described in publications [4, 5]. It consists in analyzing the recording of sound, which is caused by applying a single mechanical impact to the edge of the resonator. In this research was used an extended method of acoustic measurements of the resonator parameters which includes such features as measuring resonator characteristics at fixed angles positions, and measuring in set of stabilized temperature values. It means that perform some imitations of electrode *X* (Fig. 4) that move along resonator edge. For this purpose, a special automatic acoustic device was developed and used, which is shown in Fig. 5.

Fig. 5. Automatic device for resonator investigation by acoustic method

This special automatic acoustic device includes a mechanism for rotating the resonator at a predetermined angle, an impact mechanism for extracting sound, a microphone, a heat-stabilizing casing, which is not shown in the figure, and a heating device. For experimental determine a functional dependency deviation of maximum *Q*-factor axis because of temperature changes, the following test parameters were set: 80 impacts in range from 0 to 180° resonator angular position at the specific stabilized temperature. This testing procedure was repeated at temperature steps in the range from 30 to 65°. Such narrow-width temperature diapason choosing is explained by the necessity to only detecting and some approximate estimating the temperature deviation of *Q*-factor and own resonance frequencies axes in resonator.

Experimental data that obtained by using such device are represented by the separate sound files for each impact (Fig. 6). Well expressed modulation in sound wave signal brings a difficulty for determine *Q*-factor by detect damping time amplitude in e times. By this reason in this paper *Q*-factor was determined by using Fourier transform as $\Delta\omega_{3dB} / \omega_{1(2)}$ [12], where $\Delta\omega_{3dB}$ – width of the peak at its 0,707 height, so-called 3 dB bandwidth.

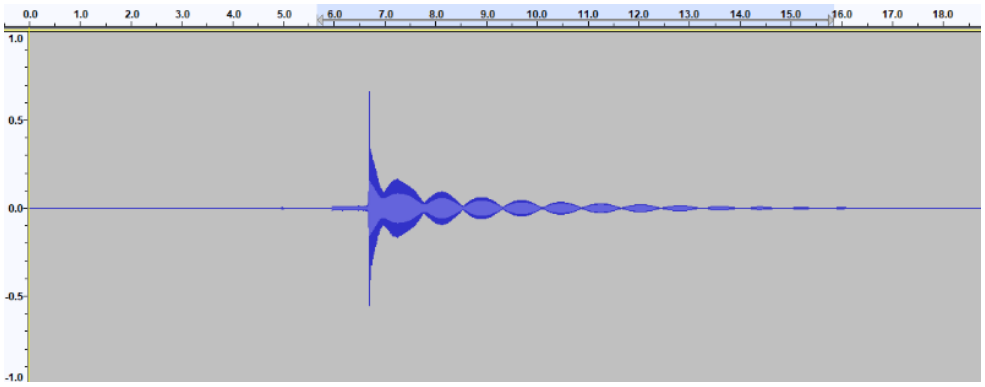

Fig. 6. Sound signal sample recorded during impact to resonator

Experimental results

As a result of the performed experimental *Q*-factor measurement by acoustic method was selected about 448 points under 8 stabilized temperature steps. Fig. 6 demonstrate a set of *Q*-factor curves for each of temperature step. Some not quite correct results noticeably for initial measurements can be explained by the not very stable conditions of the device (Fig. 5) at the start. There are pronounced four axes of *Q*-factor maximum.

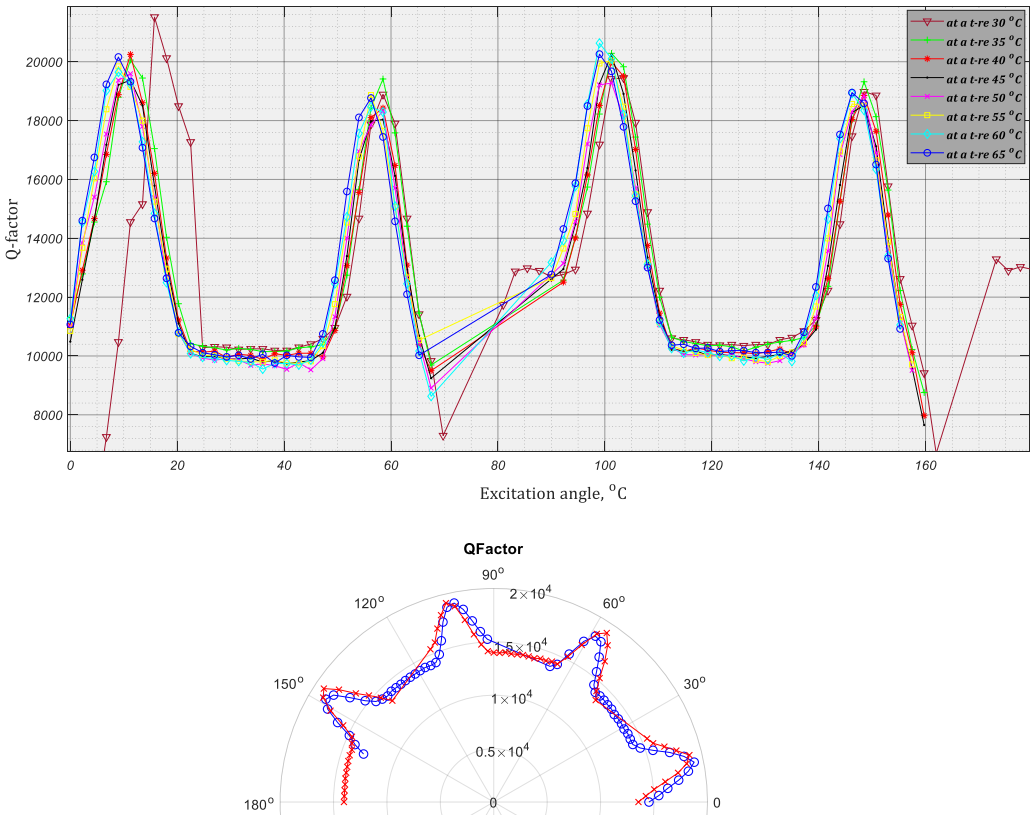

Fig. 7. *Q*-factor data under different temperature steps; *Q*-factor curve at a temperature 35°*C* in polar reference frames

Also, it visible that *Q*-factor curves have some shift relative to each other, that can be explained by *Q*-factor axes temperature drift. These axes exactly correspond with amplitudes of the sound that was obtained under impact to resonator. Experimental data shows that maximum *Q*-factor level of each splitted resonance frequency are reached when amplitudes of this frequencies are nearly equal (Fig. 8).

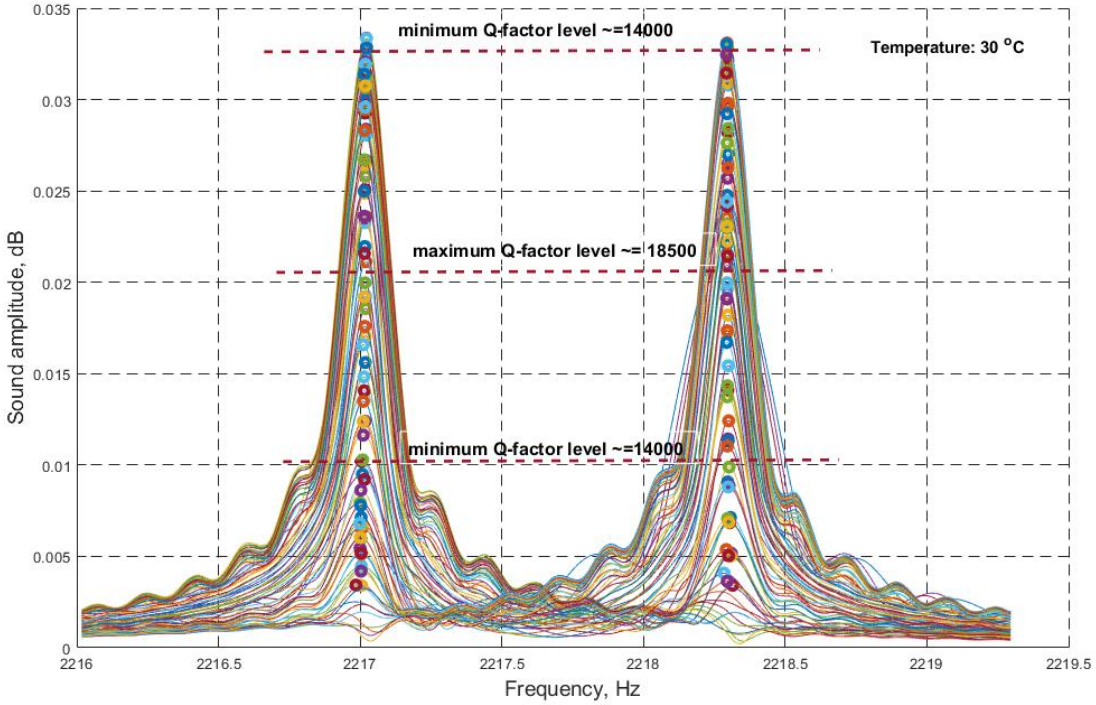

Fig. 8. *Q*-factor level distribution relate to split frequencies amplitude

It need to notice that *Q*-factor experimetnal points below to lower line "minimum *Q*-factor level" was ignored by reason of it easy validity that's why on Fig. 7 there are some missed intervals in plots. Observation of the maximum *Q*-factor level relate to sound amplitude makes possible to get more correct data of *Q*-factor axes deviation under temperature by using approximation of amplitudes of two split frequencies intersections like it shown on Fig. 9. Such approximation needs by reason that *Q*-factor experimental data have a low similar with sinusoidal form in same time as amplitude data are very close to sine-shape signal.

Fig. 9 show four well expressed frequency axes in full accordance with Fig. 2. Hence comparing this figure with Fig. 7 it is ultimate-definite that intersections ω_1 and ω_2 amplitudes are correspond with maximum *Q*-factor axes that was obtained in result of performed this acoustic method. Opposite to *Q*-factor and Sound amplitude data resonance frequencies data haven't any well-expressed dependencies from angle of impact (Fig. 10) that can help to determine temperature drifts.

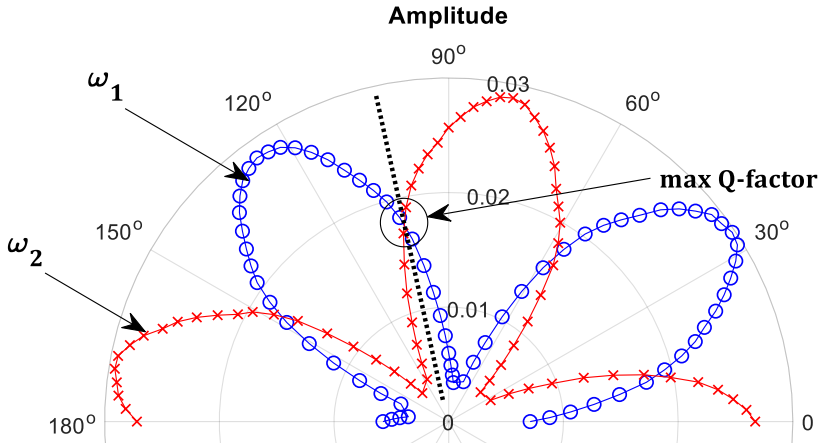

Fig. 9. Amplitude curve at a temperature 35°*C* in polar reference frames

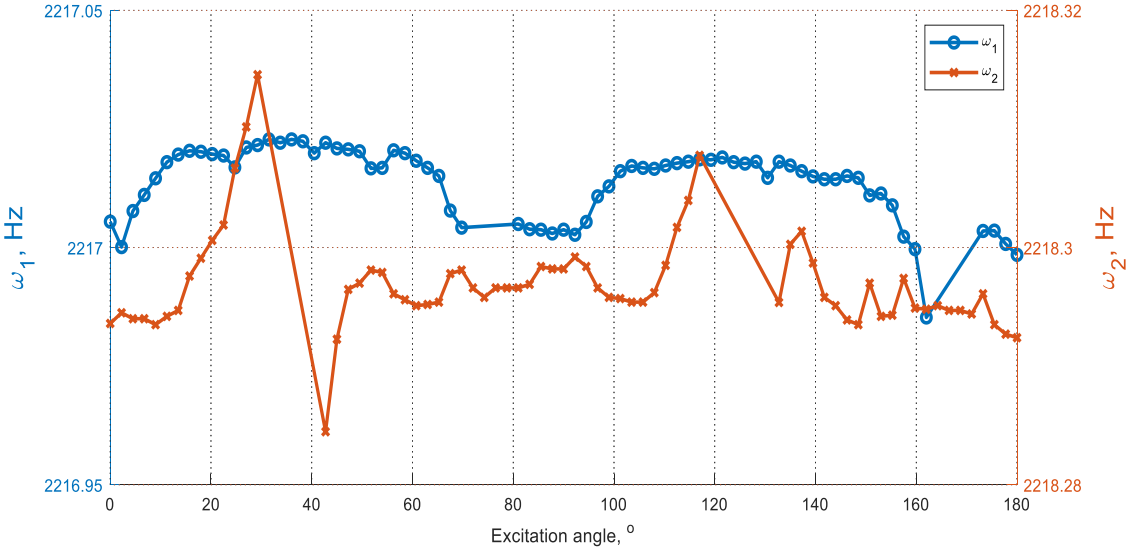

Fig. 10. Resonance split frequencies relate to angle of impact under 35°*C* temperature

As was mentioned in methodology of this extended acoustic method 80 acoustic measurements performed during one of the temperature steps in range of 0 … 180° resonator turn. It means that angle step between measurements is 2,25°. This value is very rough for direct *Q*-factor axes temperature deviation determines. By this reason was created special algorithm for more accuracy estimation of such axes move. Such algorithm include sine approximation of the *Q*-factor data with high level of validity (near the picks), sine approximation sound amplitudes, determination of amplitude curves point of exactly intersection and finally obtained values filtration. The results shows obvious all four *Q*-factor axes temperature deviations. It's approximately value about 0,079 °/°*C* with standard deviation 0,014 K/°.

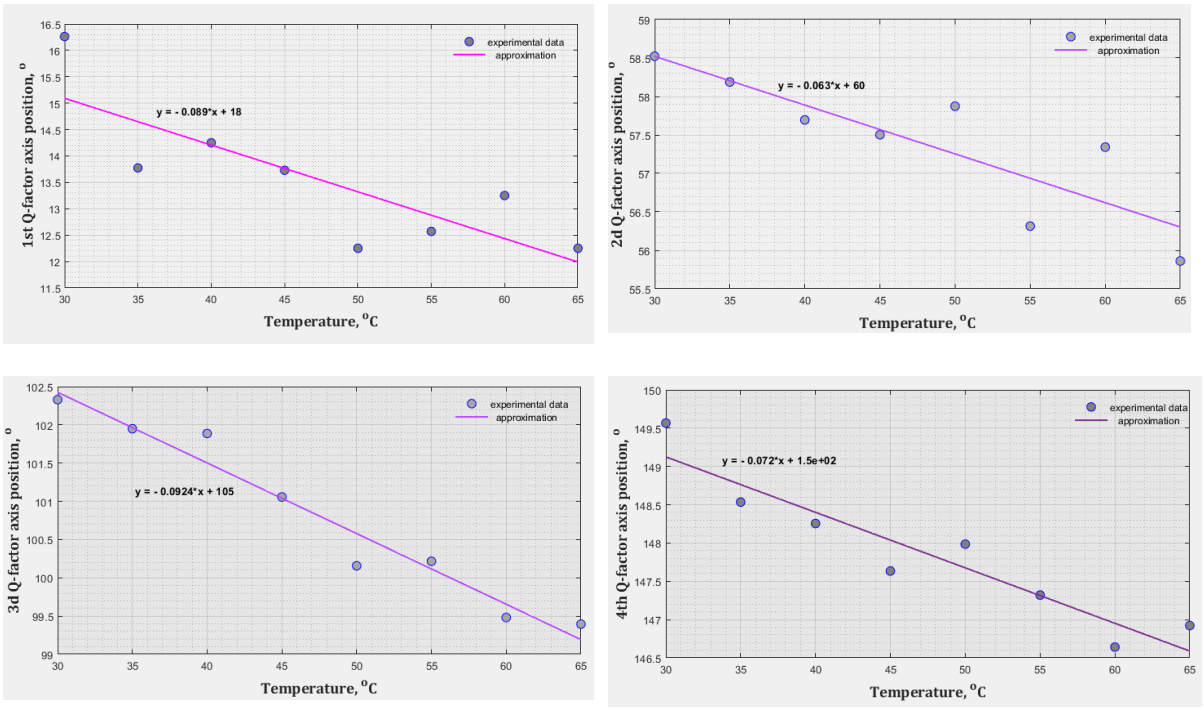

Fig. 11. Maximum Q-factor axes temperature deviation estimates

Conclusions

Extended acoustic method consider in this paper is only attempt to detect and estimate temperature deviation of such important parameter for future gyro sensor as maximum *Q*-factor axes deviation under temperature influences. Investigated method is enough rough in due to a number of objective reasons. Main reason is that detected temperature deviation is about 0,08°/°C when minimal angle of resonator excitation step is 2,25°. But in combination with post processing This method gave a quite reliable data because of them similarity for each of maximum *Q*-factor axis. The most advantages of this method is it accessibility in conditions of absence a high cost interferometric measuring equipment.

Despite a well-founded theoretical base that describe the position of own resonance axes and damping axes in metallic resonator with split resonance frequency experimental data with simple metallic resonator without electrodes obtained in this paper give additional knowledge about it behaviors in temperature and relations within acoustical data.

Investigations of the maximum *Q*-factor axes temperature deviation lead to detect evident trends with determine its values. Determined value 0,079°/°*C* is significant for CVG operating range from -40 to +70°C and it mean that correction system based on model of maximum *Q*-factor axes temperature deviation potentially can raise total CVG accuracy. Of course, such a model in the future should be built on the base of data obtained by excitation by using

electrodes after balancing, when metallic resonator will be a part of sensitive element assembly.

References

1. *Chikovani V., Okon I., Barabashov A.*, and *Tewksbury P*. A set of high accuracy low cost metallic resonator CVG, In Proceedings of 2008 IEEE/ION Position, Location and Navigation Symposium; p. 238–243.
2. *Qiu Z., Qu T., Pan Y., Jia Y., Fan Z., Yang K., Yuan J.*, and *Luo H*. Optical and Electrical Method Characterizing the Dynamic Behavior of the Fused Silica Cylindrical Resonator, Sensors. 2019, 19, 2928.
3. *Luo Y*. Dynamic Response and Frequency Split Predictions for Cylindrical Fused Silica Resonators, IEEE Sensors Journal, vol. 20, no. 7, p. 3460-3468, 2020.
4. *Цірук В. Г*. Визначення параметрів металевого резонатора вібраційного гіроскопа акустичним методом /В. Г. Цірук // Вісник Черкаського державного технологічного університету . — 2018. — № 3. — С. 74-79.
5. *Karachun V. V., Mel'nik V. N*. Determining gyroscopic integrator errors due to diffraction of sound waves. International Applied Mechanics. 2004. № 3. С. 328–336.
6. *Чиковани В. В., Яценко Ю. А*. Исследования точности измерения азимута кориолисовым вибрационным гироскопом с металлическим резонатором // XVII Санкт-Петербургская международная конференция по интегрированным навигационным системам. Сборник материалов. СПб.: ГНЦ РФ ЦНИИ «Электроприбор», 2010. С. 26–31.
7. *Chikovani V., Golovach S*. Rate Vibratory Gyroscopes bias minimization by the standing wave angle installation. 2020 IEEE 40 th International Conference on Electronics and Nanotechnology (ELNANO). 2020. p. 706-709.
8. *Матвеев В. А*. Навигационные системы на волновых твердотельных гироскопах/ В. А. Матвеев, Б. С. Лунин, М. А. Басараб. // Физматлит. – 2008. – 240 с.
9. *Журавлев В. Ф., Климов Д. М*. Волновой твердотельный гироскоп. - М.: Наука, 1985.
10. *Матвеев В. А., Липатников В. И., Алехин А. В*. Проектирование волнового твердотельного гироскопа. – М.: Изд-во МГТУ им. Н. Э. Баумана, 1997.
11. *Lynch D. D*. Vibratory gyro analysis by the method of averaging, in 2-nd Saint Petersburg International Conference on Gyroscopic Technology and Navigation, p. 26–34, St. Petersburg, Russia, 1995.
12. *Бидерман В. Л.* Теория механических колебаний. — Высшая школа, 1980. — 408 с.